

Carbon 1s near-edge-absorption fine structure in graphite

P. E. Batson

IBM Thomas J. Watson Research Center, Yorktown Heights, New York 10598

(Received 7 April 1993)

High-resolution p_z - and $p_{x,y}$ -projected fine structure for the 1s carbon core level in graphite are compared with symmetry-projected calculations. A very sharp transition occurs about 7.6 eV above the Fermi energy in the $p_{x,y}$ results, agreeing closely with the nondispersive σ^* band. An additional feature near 8.5 eV above the Fermi energy may be due to the Γ_2^- branch of the free-electron-like interlayer states. With a modest excitonic distortion, the p_z results agree closely with the expected π^* band.

Graphite has long been of interest as a prototypical anisotropic electronic material. The separation of conduction states into π^* and σ^* bands has been verified with many techniques over the years. Holzwarth, Louie, and Rabii¹ and Posternak *et al.*² suggested that a free-electron-like set of bands, corresponding to electronic excitations lying between the graphite layers (interlayer states), may exist in the pristine material. These had been observed in alkali-intercalated graphite and were thought not to exist in graphite alone.³ Evidence for these states was then found using angle-resolved inverse photoemission.⁴ Recently a study using synchrotron x-ray-absorption fine structure has also found positive evidence for these states, but with some disagreement as to the position of the interlayer states relative to the Fermi energy.⁵

I report here high-resolution absorption spectroscopy, using inelastic electron scattering in transmission at high energy of the carbon $1s \rightarrow \pi^*$ and σ^* states. By using a 1-nm-sized beam in a scanning transmission electron microscope (STEM), an area of single-crystal, well-oriented graphite can be probed. By comparing results using different angular collection ranges, fine structure relating to p_z and $p_{x,y}$ directions can be separated. The energy resolution ranged from 0.15 to 0.22 eV, depending on the statistical quality of the data. I find a nearly resolution-limited peak at the σ^* position corresponding to a flat-band lying in the Γ - M - L - A planes. There does not appear to be any structure between the π^* and σ^* peaks, but there is unidentified structure just above the sharp σ^* peak. This structure is consistent with the presence of a dipole-allowed free-electron-like band dispersing from just above the σ^* transition. I suggest that this is the Γ_2^- interlayer band.

These experiments used 50–80-nm-thick areas of single-crystal Ticonderoga graphite. The sample areas were chosen to be flat and oriented so that the c axis was parallel to the incident-beam direction. The VG Microscopes HB501 scanning transmission electron microscope, fitted with a high-resolution Wien filter electron spectrometer, has been described elsewhere.⁶ A power-law background has been stripped from the carbon 1s spectra. Next, the experimentally measured, 0.4-eV-wide, field-emission distribution has been unfolded from the data to reveal structure at the 0.15–0.22-eV level, de-

pending on the statistical quality of the data. This step is made possible by the 70–150-meV resolution of the spectrometer and is crucial due to the lack of an electron source monochromator. The procedure for doing this has been explained in detail elsewhere.⁷

I show in Fig. 1 the background stripped data, the sharpened data, and an inset summarizing the modification of the resolution function from the 0.4-eV-wide field-emission distribution to a symmetric function having a width of 0.171 eV. The sharpened curve summarizes results for 0.17-eV (line) and 0.22-eV resolution (dots). Small fluctuations of intensity are the result of noise amplification by the resolution sharpening process. The limiting width of the sharp σ^* peak is about 0.35 eV, while the width of the π^* peak remains 1.05 eV. The π^* peak position is 285.38 ± 0.05 eV in good agreement with previous experimental results.⁸ As is obvious from the data, there are no peaks evident in the region between the π^* and σ^* structures. This result was obtained with an 8-mrad half-angle convergence, to form a 1-nm probe, and using all scattering out to 10-mrad half-angle collec-

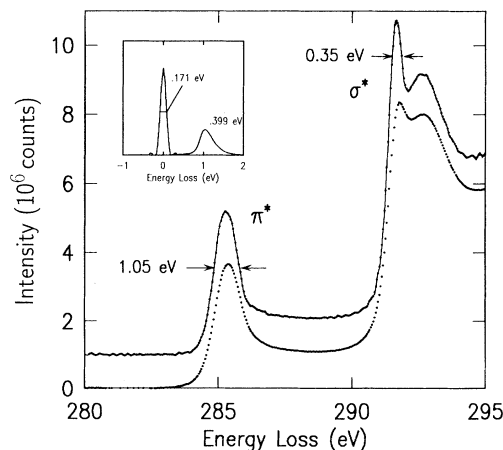


FIG. 1. Comparison of the raw data (lower curve) with results of resolution sharpening to 0.171 eV (upper line) and 0.22 eV (dots). The inset shows the effective no-loss energy distribution enhancement from the 0.399-eV-wide asymmetric field-emission distribution to a 0.171-eV-wide nearly Gaussian distribution.

tion limit. Therefore, the spectra are integrated over perpendicular momentum transfer out to a maximum of about 1.76 \AA^{-1} . This scattering geometry mostly confines the scattering wave vector to lie in the plane perpendicular to the incident beam—in this case the a, b plane of the graphite. The ratio of π^* to σ^* intensity is typical for these conditions in the spatially resolved experiment when imaging is a primary objective. In this case, the imaging capability ensures that the graphite was a single crystal, oriented correctly, and did not have large amounts of surface contamination.

In Fig. 2, I compare results using two different angular collection ranges. In a small-angle scattering experiment, when the perpendicular momentum transfer is small relative to the parallel momentum transfer defined by the energy loss, the momentum transfer has a large component that is parallel to the incident-beam direction—in this case along the graphite c axis. I used a nearly parallel incident beam and a collection half angle of 2 mrad. This gives $q_{\perp} = 0.3 \text{ \AA}^{-1}$ while $q_{\parallel} \approx K_0 \Delta E / 2E_0 = 0.24 \text{ \AA}^{-1}$, where $K_0 = 176 \text{ \AA}^{-1}$ is the incident momentum for the incident energy $E_0 = 100 \text{ keV}$. This result more nearly resembles dedicated angle-resolved electron-energy-loss spectroscopy (EELS) experiments.⁹ From the symmetry-projected density-of-state (DOS) calculations, we expect that the peak at 285.38 eV is comprised entirely of contributions from the π^* final states. If the π^* peak from the large- and small-angle measurements are normalized, we may subtract these data to obtain scattering

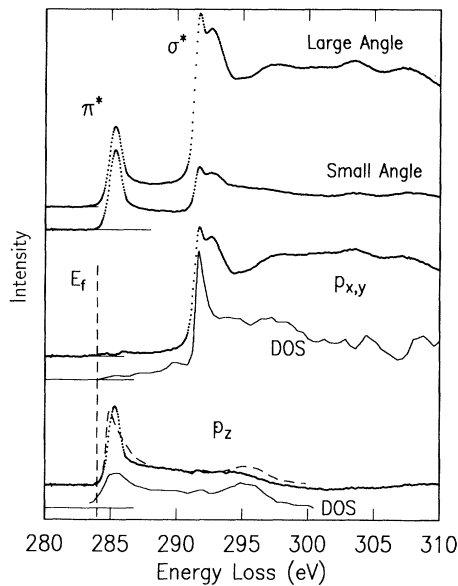


FIG. 2. In the upper section, data from large and small collection apertures are displayed with the π^* peaks normalized. In the middle section the $p_{x,y}$ component, obtained by subtraction from the upper panel data, is compared with the $p_{x,y}$ DOS from Ref. 11. In the bottom panel, the p_z data, obtained by subtraction of the $p_{x,y}$ results from the large-angle data, are compared with the p_z DOS from Ref. 11. Good agreement is obtained with a small excitonic enhancement (dashed line).

due only to the $p_{x,y}$ final states, as shown in Fig. 2. This procedure is similar to the analysis described by Browning, Yuan, and Brown.¹⁰ Further, since the major part of the π^* band is expected to end at a band maximum near 295 eV, we may normalize the $p_{x,y}$ result to the large-angle result between 305 and 315 eV and subtract to obtain only the p_z final states. This procedure completely separates the π^* and σ^* structure. In the prior work, a different separation was obtained using different assumptions relating to the absolute scattering intensity using different integration apertures.¹⁰ Application of those assumptions to these data gives a similar separation.

The results are compared in Fig. 2 with the $p_{x,y}$ - and p_z -projected calculation of Weng, Rez, and Ma,¹¹ after aligning the sharp σ^* peak to the data at 291.65 eV. I place the Fermi level at 284 eV in agreement with earlier work.⁸ There is also good alignment with the position and width of the π^* band (within 0.2 eV), although a discrepancy in intensity still exists. I have investigated adding a small excitonic enhancement to improve the agreement, and find that a 0.1-eV excitonic binding energy, using a weak Wannier exciton model¹² with some modification,¹³ is sufficient to reproduce the position and height of the π^* peak. This improves on the 2-eV binding energy needed previously using a DOS calculated for only a single layer of graphite.⁸

Clearly, from the $p_{x,y}$ result, the σ^* peak is resolved into two components, a very sharp peak at 291.65 eV and a broader feature near 292.5 eV. The second feature does not appear to be strongly represented in the calculation. On the other hand, the weak feature near 290 eV in the calculation is not present in the data. In Fig. 3 I show an expanded region of the $p_{x,y}$ scattering near 291 eV at an energy resolution of about 0.15 eV. For a comparison, I have constructed a trial DOS consisting of two contributions. The first is a Gaussian-shaped peak centered at 291.65 eV having a full width of 0.4 eV. The second is a free-electron-like contribution having a dipole-allowed onset at 291.9 eV, increasing to higher energy with a

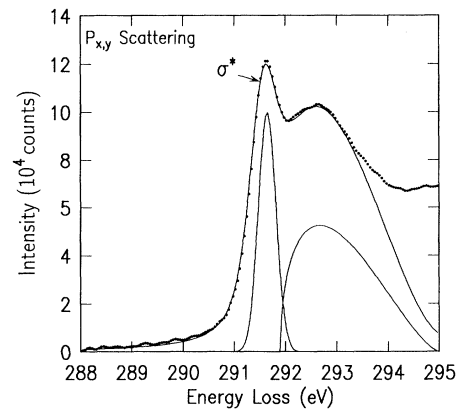


FIG. 3. Detailed region of the σ^* data at 0.15-eV resolution. The data can be understood to result from two contributions: (i) a very sharp σ^* peak at 291.65 eV and (ii) a bandlike contribution having an onset at 291.9 eV and an initial square-root energy dependence.

square-root energy dependence, but approaching a dipole-forbidden band maximum near 295 eV. This shape has been useful in understanding details of the dipole-allowed DOS in silicon.¹⁴ In this case, I assume that the Γ_2^- allowed transition becomes dipole forbidden near the Brillouin-zone boundaries at K and M . To compare with the measured data, I have convolved with a 0.2-eV-wide Lorentz shape to approximate core-hole lifetime damping, and with a 0.15-eV-wide Gaussian for the instrumental resolution. Clearly, all of the intensity below 291 eV can be attributed to lifetime broadening of the σ^* scattering.

In conclusion, the carbon 1s core absorption in graphite has been obtained with high-energy resolution, and has been resolved into $p_{x,y}$ and p_z components. Agree-

ment with calculations is very good except for the presence of a broad feature in the $p_{x,y}$ results near the sharp σ^* peak. This feature is consistent with a dipole-allowed, dispersive transition which may be related to the Γ_2^- branch of the interlayer states as proposed by Posternak *et al.*² This result is consistent with the work of Fauster *et al.*⁴ who found a dispersive state between the π^* and σ^* bands in the pristine graphite, corresponding to the s -like Γ_1^+ interlayer state. It does not obtain a peak located below the σ^* transition as was noticed in x-ray-absorption measurements of highly oriented polycrystalline (HOPG) and polycrystalline graphite.⁵

I want to acknowledge useful discussions with P. Rez and N. D. Browning during this work.

¹N. A. Holzwarth, S. G. Louie, and S. Rabii, *Phys. Rev. B* **26**, 5382 (1982).

²M. Posternak, A. Baldereschi, A. J. Freeman, E. Wimmer, and M. Weinert, *Phys. Rev. Lett.* **50**, 761 (1983).

³P. Pfluger and H. J. Guntherodt, in *Festkörperprobleme: Advances in Solid State Physics*, edited by J. Treusch (Vieweg, Braunschweig, 1981), Vol. 21, p. 271, and references therein.

⁴T. Fauster, F. J. Himpsel, J. E. Fisher, and E. W. Plummer, *Phys. Rev. Lett.* **51**, 430 (1983).

⁵D. A. Fischer, R. M. Wentzcovitch, R. G. Carr, A. Cotinzenza, and A. J. Freeman, *Phys. Rev. B* **44**, 1427 (1991).

⁶P. E. Batson, *Rev. Sci. Instrum.* **57**, 43 (1986); **59**, 1132 (1988).

⁷P. E. Batson, D. W. Johnson, and J. C. H. Spence, *Ultramicroscopy* **41**, 137 (1992).

⁸E. J. Mele and J. J. Ritsko, *Phys. Rev. Lett.* **43**, 68 (1979).

⁹B. M. Kincaid, A. E. Meixner, and P. M. Platzman, *Phys. Rev. Lett.* **40**, 1296 (1978).

¹⁰N. D. Browning, J. Yuan, and L. M. Brown, *Ultramicroscopy* **38**, 291 (1991); *Philos. Mag.* **67**, 261 (1973).

¹¹X. Weng, P. Rez, and H. Ma, *Phys. Rev. B* **40**, 4175 (1989).

¹²R. J. Elliott, *Phys. Rev.* **108**, 1384 (1957).

¹³P. E. Batson and J. Bruley, *Phys. Rev. Lett.* **67**, 350 (1991).

¹⁴P. E. Batson, *Ultramicroscopy* **50**, 1 (1993).